# Global measurement of Reynolds stress in a cylindrical linear plasma

Y. Nagashima[1], S. –I. Itoh[1], S. Inagaki[1], S. Oldenbürger[1], T. Kobayashi[1], K. Kawashima[1], N. Ohyama[1], Y. Tobimatsu[1], S. Yamada[1], T. Yamashita[1], H. Arakawa[2], K. Kamataki[1], T. Yamada[3], M. Sasaki[1], N. Kasuya[4], M. Yagi[2], A. Fujisawa[1], P. H. Diamond[4], and K. Itoh[5]

[1]*Kyushu University, Kasuga, Japan*

[2]*Naka Fusion Institute, Japan Atomic Energy Agency, Naka, Japan*

[3]*Graduate School of Frontier Sciences, the University of Tokyo, Kashiwa, Japan*

[4] *University of California San Diego, La Jolla, USA, Toki, Japan*

[5] *National Institute for Fusion Science*

**1. Introduction**: Recent experimental studies have clarified the mechanism behind the generation of global fields (momentum and magnetic fields) by turbulence, in the aspect of statistical average. However, further investigations are necessary for understanding of dynamic behaviour of fluctuations, in case of far-non-equilibrium states of plasmas. In particular, study on stochastic process of radial electric field has been focused on in fusion research community because of its effect on transition between plasma confinement states [1]. In order to clarify the dynamics of global momentum fields excited by nonlinear force originated from micro-scale fluctuations (i.e., Reynolds stress), global and simultaneous measurements of the widely distributed momentum field and micro-scale fluctuations with a number of diagnostics are required. We have installed a probe arrays in a linear plasma device of Kyushu University. In this paper, we present results of global pattern of Reynolds stress with the probe array.

**2. Experiments**: Experiments have been conducted on a linear cylindrical plasma device, Large Mirror Device - Upgrade. Magnetic field strength *B* is fixed at 0.09 T inside the plasma column, and the ion cyclotron frequency $f_{ci}$ is 34 kHz. Filling gas pressure is about 2 mTorr. Spectrum peak of drift-wave fluctuation is observed at about 7.5 kHz and azimuthal mode number $m = 2$, and secondary instabilities has the frequency of 1-2 kHz and mode number $m = -1$, where positive *m* means propagation in the electron diamagnetic drift direction.

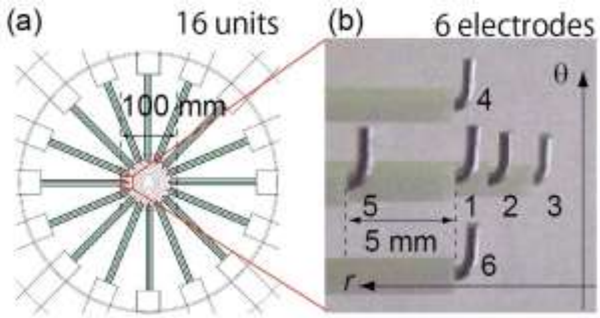


Fig. 1 (a) Arrangement of 16 units of Reynolds stress probe, and (b) enlarged view of head of a unit

The probe array [2] is composed of 16 units. Each probe unit can be radially movable, and has 6 electrodes at the head of the unit. All electrodes are used for measurement of floating potential fluctuation ($\Phi_{f,n}$, where $n$ is numbering of the electrodes). Radial and azimuthal $E \times B$ velocity fluctuations ($v_r$ and $v_\theta$) are obtained from derivatives of the floating potential fluctuation, $v_r = -(\Phi_{f,5} - \Phi_{f,3})/d_r$, and $v_r = -(\Phi_{f,4} - \Phi_{f,6})/d_\theta$. ,where $d_\theta$ and $d_r$ are gaps between the electrodes, and we also obtain Reynolds stress $-\langle v_r v_\theta \rangle$. During the experiment, the 15 probe units are fixed at $r = 4$ cm, where the local Reynolds stress has a maximum [3]. Radial location of a probe unit is scanned every discharge, and we observed radial profile of Reynolds stress with attention to check reproducibility of fluctuation phenomena.

Fourier based analysis is useful to reveal propagation and amplitude distribution of fluctuations in the aspect of statistical average. Combining auto-power and cross-phase analyses, we reconstruct two-dimensional patterns of fluctuations. Here we reconstruct the patterns by cross product of amplitude and phase information, where radial locations of 15 probe units are fixed and rest one unit is scanned. We used Reynolds stress data for the fixed probe data, and other physical quantities for the scanned data. Cross spectral analysis is performed between scanned probe and fixed probes. The amplitude is derived from square root of auto-power spectra of the scanned probe integrated over frequency, and phase information is used as cosine of the cross-phase assuming azimuthal symmetry of fluctuation amplitude. The integration range is almost the same as the frequency resolution. Thus, the two-dimensional patterns imply approximately information of frequency-wavenumber space. In particular, the patterns include two-dimensional spectra of both radial and azimuthal wave-numbers. In quasi-two-dimensional turbulence, secondary vortex structures such as zonal flows, streamers, and general Kelvin-Helmhortz instability can be generated by bunching and/or modulation of waves in radial and azimuthal wave-number spaces. Therefore, analysis of the patterns in detail will open the way for nonlinear analysis of three-dimensional (temporal, azimuthal, and radial directions) nonlinear analysis.

**3. Experimental results**: Figure 2 show the two-dimensional patterns of fluctuations at the frequency of 7.5 kHz, corresponding to the drift-wave fluctuation. Figures 2(a, b) show the oscillating patterns of Reynolds stress and potential fluctuation. The schematic view of the fixed probes and scanned probe is shown in Fig.2(c). The dimension of time derivative or damping of electrostatic potential ($\Phi/B$) is the same as that of Reynolds stress ($-\langle v_r v_\theta \rangle$). Therefore, comparison between the potential and Reynolds stress has a physical meaning in term of equation of motion. We observed spatial patterns with $m = 2$ in both the potential

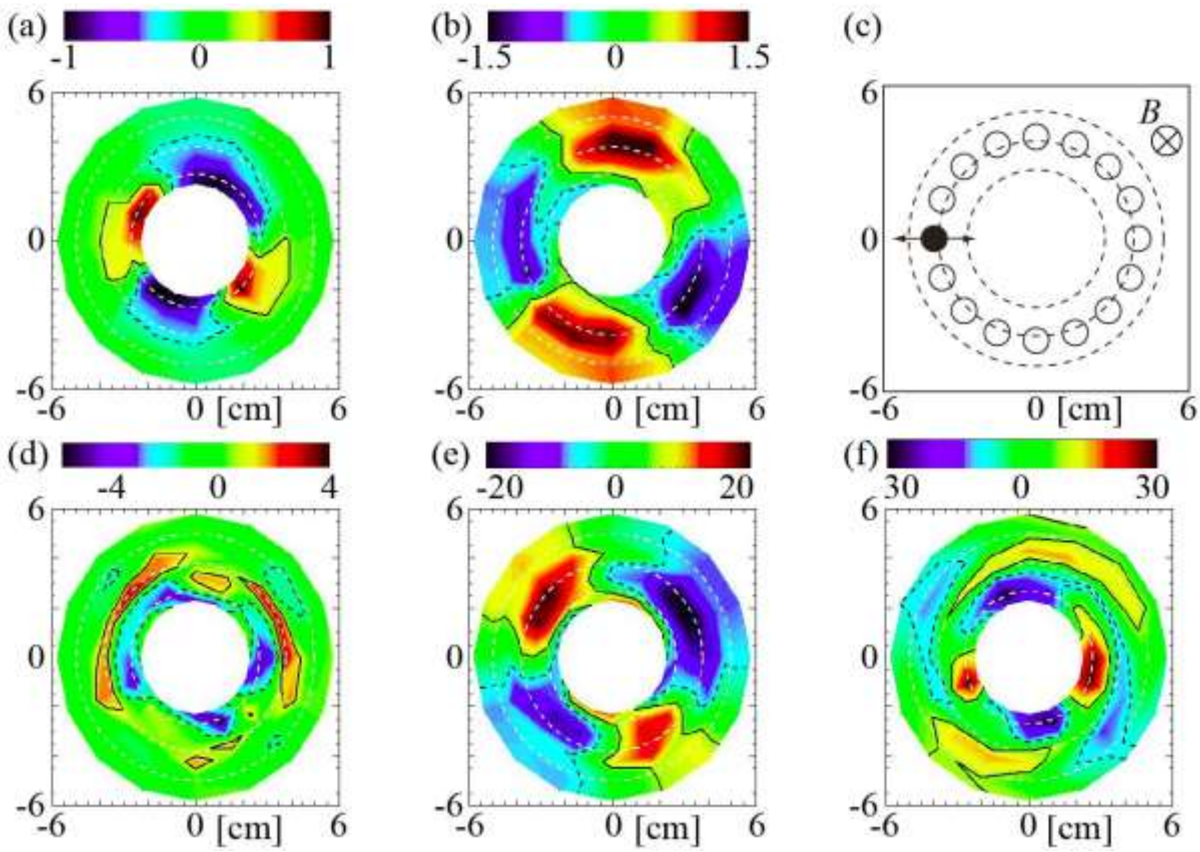


Fig. 2 Image contour plots of fluctuations in arbitrary unit. Horizontal and vertical axes indicate location on the plasma cross-section orthogonal to the magnetic field in cm unit. (a) Oscillation of Reynolds stress at 7.5 kHz, and (b) floating potential fluctuation at 7.5 kHz. (c) Schematic view of fixed and movable probe locations. Open circles indicate the fixed probe units, and a filled circle is radially movable probe. (d) Cross product of radial and azimuthal *E*x*B* velocity fluctuation. Frequency of the velocity fluctuations is 7.5 kHz. (e, f) Azimuthal and radial electric field fluctuations at 7.5 kHz. In (a, b, d-f), black solid and dashed lines emphasize positive and negative boundary of fluctuation polarities. Three white dashed lines show radial locations at 5.0, 3.8, and 2.7 cm, respectively. In (c), the same circular dashed lines are drawn in black. There is no data of fixed probe at the scanned probe unit, and the data are interpolated.

fluctuation and oscillation of the Reynolds stress. However, the phase relationship between them is out of phase. This result suggests that the oscillation of the Reynolds stress may contribute reduction of the drift wave potential. This result can be understood considering modulational instabilities. When the modulatinal instability may generate a secondary instability and two sidebands of the drift wave, pairs of the primary drift wave and one of the sidebands generate the secondary instability in the nonlinear equations. On the contrary, pairs of the secondary instability and the sidebands reduce the primary drift wave energy. Oscillation of the Reynolds stress could be composed of the secondary instability and the sidebands. It should be noted that Reynolds stress is not the unique nonlinear source/sink for the drift wave potential. Spatial inhomogeneity of compression of momentum could contribute generation/reduction for fluctuation, therefore, total contribution of the nonlinear force to generation/reduction of the drift-wave potential is not conclusive.

Figure 2(d-f) shows two-dimensional profiles of stationary Reynolds stress (RS) and patterns of electric field fluctuations. In Fig. 2(d), the stationary RS profile is obtained by cross product of radial and azimuthal electric fields fluctuations at 7.5 kHz. Therefore, the stationary RS is mainly composed of the primary drift wave including sidebands whose frequencies are very close to the frequency of the primary drift wave. The sidebands could contribute to generation of very low frequency secondary instability such as zonal flows. Azimuthal mode structure of the stationary RS is weak ($m$ = 0 is dominant, including small amplitudes of finite $m$ numbers), but we can observe significant radial gradient of the stationary RS just inside $r$ = 3.8 cm. Figure 2(d) shows that the stationary RS gradient remains even after averaging over the azimuthal direction [3], and can contribute generation of global momentum field. This is the first measurement of the global (radial and azimuthal) RS structure with the probe array. This also implies that the modulational instability between the shear flow and drift-waves may occur. The radial wave number modulation is also observed as the wave front bending of the potential fluctuation at around $r$ = 3.8 cm in Fig. 2(b). The physical picture behind the modulational instability can be understood by considering Fig. 2(e, f). The azimuthal electric field fluctuation in Fig. 2(e), corresponding to the radial $E\times B$ velocity fluctuation, has a clear azimuthal mode structure $m$ = 2 with the bending of the wave front as seen in Fig. 2(b). On the contrary, the radial electric field fluctuation in Fig. 2(f), corresponding to the azimuthal $E\times B$ velocity fluctuation, also has clear $m$ = 2 structure, but the wave phase patterns are significantly stretched in the azimuthal direction, and have complicated spiral structure, indicating that vortex tilting of the drift wave fluctuation, a candidate for the generation mechanism of zonal flows, may occur. We need further analyses, experiments, and upgrade of diagnostics in the next linear device PANTA [4] for understanding global and dynamical picture behind the coexistence of multi-scale fluctuation. These experiments open the way for exploring the physics picture.

**Acknowledgement**: This work is partly supported by grants-in-aid for scientific research of JSPF, Japan (21224014, 23360409) and by the collaboration programs of NIFS and of the RIAM of Kyushu University and Asada Science foundation.

## References

[1] S. –I. Itoh, et al., Physical Review Letters 89 (2002) 215001
[2] Y. Nagashima, et al., Review of Scientific Instruments 82 (2011) 033503
[3] Y. Nagashima, et al., Physics of Plasmas 18 (2011) 070701
[4] S. Oldenbürger, et al., Plasma Physics and Controlled Fusion 54 (2012) 055002